Arrays of Bodies of Revolution for Minimum Wave Drag

Jack N. Nielsen*
NASA Ames Research Center, Moffett Field, California

The wave drag of two identical Sears-Haack bodies at transonic and supersonic speeds has been determined by using the supersonic area rule. The solution is found for these bodies displaced parallel to each other, both laterally and longitudinally. The results show that the drag of a pair of bodies can be either doubled, or nearly halved, depending upon the lateral and longitudinal spacings of the bodies. The magnitude of this drag is determined by the degree of mutual interference between the bodies. It is shown how reductions in wave drag can be obtained by proper spacing of external bodies. The regions of favorable mutual interference are delineated. It is also shown how to apply the two-body results to many-body arrays. Some remarks are made on applying the results to store-airframe interference and on further aspects of the store-airframe drag problem.

Nomenclature

a = half the lateral spacing between two bodies of revolution displaced parallel to one another
b = the longitudinal spacing between two bodies of revolution displaced parallel to one another
C_D = $D/q_\infty S_R$
C_{D_I} = $D_I/q_\infty S_R$
ΔC_D = drag coefficient resulting from mutual interference between Sears-Haack bodies
D = wave drag of a number of identical Sears-Haack bodies
D_I = wave drag of body B_I alone
D_2 = wave drag of body B_2 alone
f = $a\beta\cos\epsilon$
I_1,I_2,I_3,I_4 = drag integrals in the supersonic area rule; see Eqs. (13), (16), (17), and (14), respectively
J = definite integral defined by Eq. (24)
K_0,K_1 = definite integrals defined by Eqs. (32) and (33), respectively
L = length of body of revolution
M = definite integral given by Eq. (38)
M_∞ = freestream Mach number
n = any integer; also number of similar bodies of revolution
N = definite integral given by Eq. (39)
q_∞ = freestream dynamic pressure
R = definite integral given by Eq. (43)
r = radius of body of revolution
r_0 = maximum radius of body of revolution
S = cross-sectional area of body of revolution
S_I = S for body B_I
S_2 = S for body B_2
S_R = reference area, πr_0^2
t = $\lambda+\cos\phi$
x,y,z = set of Cartesian coordinates, x rearward, y horizontal to the right, and z vertically upward
x_0 = value of x for apex of Mach cone
β = $(M_\infty^2-1)^{1/2}$
γ = $\cos^{-1}(\cos\phi+\lambda)$
ϵ = polar angle of plane tangent to Mach cone
η = $\xi+(b/L-f)$; Eq. (12)
θ = position variable for body x station; Eq. (1)
λ = $2(b-2f)/L$
ξ = dummy variable of integration
τ = $(b/L-f)$, Eq. (12)
ϕ = position variable for body η station, Eq. (23)

Received Dec. 4, 1984; presented as Paper 85-0449 at the AIAA 23rd Aerospace Sciences Meeting, Reno, NV, Jan. 14-17, 1985; revision received April 25, 1985. This paper is declared a work of the U.S. Government and therefore is in the public domain.

*Chief Scientist. AIAA Fellow.

Introduction

CURRENTLY, there is much interest in reducing the drag of external stores by properly integrating the airplane and stores to meet this end. One reason for this interest is that a supersonic airplane with pylon-mounted stores can generate sufficient drag to preclude supersonic flight. This is particularly true when utilizing triple ejection racks or multiple ejection racks. This paper will show that this excessive wave drag can be reduced. The basic purpose of this paper is to show how, at transonic and supersonic speeds, mutual interference between identical stores can be harnessed to reduce the wave drag caused by these stores. In addition to external stores, the paper has application to twin-body aircraft.

The drag of an isolated store consists of the body wave drag, body skin friction, base drag, and empennage drag, although the latter two quantities are zero for a body of revolution with a pointed base. When mounted alone on an aircraft, an external store has a drag increment due to the interference of the airplane on the store. The airplane also has a drag increment due to the effect of the store on the airplane. When multiple arrays of stores are mounted on the airplane, there is mutual interference among the stores. Methods exist generally for calculating the wave drag, skin friction, and base drag of isolated bodies of revolution. However, methods for calculating the wave drag due to mutual interference between bodies have not been widely applied. It will be shown that large savings in wave drag are to be gained by the favorable use of mutual interference.

Several methods exist for determining the wave drag of combinations of bodies of revolution. First there are panel methods such as PAN AIR.[1] These methods will yield the wave drag, but they are limited practically to only a few bodies because of the large number of panels required. Area rule methods[2] are also applicable. It will be shown that once the two-body problem is solved, it can be applied to the multiple-body problem. In addition, the area rule method gives algebraic answers in closed form in many instances. In these cases the singularities are handled exactly from the mathematical point of view.

In Ref. 3, Drougge reports a combined experimental-theoretical study of parabolic-arc bodies at transonic speeds.

The experimental results are pressure distributions and total drags for a parabolic-arc body (truncated) in the presence of another similar body. The bodies have been truncated to 5/6 of the total length of a parabolic-arc body to accommodate the supporting stings. The force measurements include skin friction. Theoretical results based on the supersonic area rule are derived. The theoretical results do not apply to a body the nose of which lies behind the Mach forecone of the trailing edge of the forward body. As such, they cannot be used to estimate the wave drag of most multiple arrays of bodies. The present results for Sears-Haack bodies (which are pointed at both ends) are not so limited. Parabolic-arc bodies have 6% more wave drag than Sears-Haack bodies for the same length and volume.

Derivation of Drag Integral

The supersonic area rule method will be applied to two Sears-Haack bodies which are displaced parallel to each other in both the lateral and longitudinal directions.

Consider first the following notation and results for a Sears-Haack body taken from Ref. 2, pp. 281-283. Introduce the angle θ such that

$$x/L = (1+\cos\theta)/2 \tag{1}$$

for body 1 with $\theta = 0$ corresponding to the trailing edge of the body and $\theta = \pi$ corresponding to the point of the nose. The cross-sectional area distribution is given in terms of θ as

$$S_1(\theta) = \pi r_0^2 \sin^3\theta \tag{2}$$

The drag based on πr_0^2 as reference area is

$$C_{D_1} = \frac{9}{2}\pi^2 (r_0/L)^2 \tag{3}$$

A quantity that will be used later is

$$S_1'' = \frac{d^2 S_1}{dx^2} = 12\pi \frac{r_0^2 \cos 2\theta}{L^2 \sin\theta} \tag{4}$$

In the supersonic area rule the idea of a plane tangent to the Mach cone is used. Consider such a plane tangent at polar angle ϵ to a Mach cone with origin at x_0. The plane has the equation

$$x - x_0 = \beta y \cos\epsilon + \beta z \sin\epsilon \tag{5}$$

In the plane $z = 0$ with $y = a$

$$x = x_0 + \beta a \cos\epsilon = x_0 + f \tag{6}$$

Consider now two bodies of revolution separated laterally by distance $2a$ and longitudinally by distance b. Let a Mach cone travel along the x axis with the tangent plane cutting oblique cross-sectional areas from body B_1 and body B_2. The projections of these oblique areas on a plane normal to the axis x are very closely equal to $S_1(x_0 - f)$ and $S_2(x_0 + f)$, respectively.

In applying the supersonic area rule to the combination of two bodies, the Mach cone and its tangent plane range along the x axis between the limits for which the tangent plane can intersect bodies B_1 and B_2. It is convenient to fix ϵ, and hence the limits of integration for the first double integration, and then to averge over ϵ in the third integration. The drag expression for fixed ϵ is

$$\frac{d}{d\epsilon}\left(\frac{D}{q_\infty}\right) = -\frac{1}{2\pi}\int\int S''(x) S''(\xi) \ln|x-\xi| \, dx\, d\xi \tag{7}$$

Here S includes area intercepted from both bodies by the tangent plane at angle ϵ, and the limits cover all x and ξ for which S'' is not zero. The total drag is

$$\frac{D}{q_\infty} = \frac{1}{2\pi}\int_0^{2\pi} \frac{d}{d\epsilon}\left(\frac{D}{q_\infty}\right) d\epsilon \tag{8}$$

Let

$$S(x) = S_1(x) + S_2(x) \tag{9}$$

so that

$$S''(x)S''(\xi) = S_1''(x)S_1''(\xi) + S_1''(x)S_2''(\xi) + S_1''(\xi)S_2''(x) + S_2''(\xi)S_2''(x) \tag{10}$$

and Eq. (7) expands to four integrals. It is noted that x ranges from $-(b/L-f)$ and $L-(b/L-f)$ for B_1. (Fig. 1) and between $(b/L-f)$ and $L+(b/L-f)$ for B_2. The first term of Eq. (10) yields the integral

$$I_1 = -\frac{1}{2\pi}\int_{-(b/L-f)}^{L-(b/L-f)} S_1''(x)\,dx \int_{-(b/L-f)}^{L-(b/L-f)} \times S_1''(\xi) \ln|x-\xi| \, d\xi \tag{11}$$

Let

$$\tau = x + \left(\frac{b}{L} - f\right), \qquad \eta = \xi + \left(\frac{b}{L} - f\right) \tag{12}$$

Then

$$I_1 = -\frac{1}{2\pi}\int_0^L \int_0^L S_1''(\tau) S_1''(\eta) \ln|\tau - \eta| \, d\tau\, d\eta \tag{13}$$

In the equations, $S_1''(x)$ and $S_1''(\xi)$ range over their values from the nose to the trailing edge of the body. Formally the transformation $S_1(x) \to S_1(\tau - (b/L) + f)$ should appear in Eq. (13). With the understanding that $S_1(x)$ ranges over the same values in both equations and is given by Eq. (2), Eq. (13) can be written in its present form for convenience. The integral I_1 represents the drag of body B_1 by itself. Similarly, the last term of Eq. (10) yields

$$I_4 = -\frac{1}{2\pi}\int_0^L \int_0^L S_2''(\tau) S_2''(\eta) \ln|\tau - \eta| \, d\tau\, d\eta \tag{14}$$

which corresponds to the drag of body B_2 alone.

The second and third terms of Eq. (10) represent the mutual interference drag between bodies B_1 and B_2. With due regard for the different limits for S_1 and S_2,

$$I_2 = -\frac{1}{2\pi}\int_{-(b/L-f)}^{L-(b/L-f)} S_1''(x)\,dx \int_{b/L-f}^{L+(b/L-f)} S_2''(\xi) \ln|x-\xi| \, d\xi \tag{15}$$

If one makes the limits of both integrals 0 and L, the result is

$$I_2 = -\frac{1}{2\pi}\int_0^L \int_0^L S_1''(\tau) S_2''(\eta) \ln|\tau - \eta - (b-2f)| \, d\tau\, d\eta \tag{16}$$

The third integral with the appropriate limits is

$$I_3 = -\frac{1}{2\pi}\int_{b/L-f}^{L+b/L-f} S_2''(x)\,dx \int_{-(b/L-f)}^{L-(b/L-f)} S_1''(\xi) \ln|x-\xi| \, d\xi \tag{17}$$

$$I_3 = -\frac{1}{2\pi}\int_0^L \int_0^L S_2''(\tau) S_2''(\eta) \ln|\eta - \tau - (b-2f)| \, d\tau\, d\eta \tag{18}$$

Reversing the dummy variable of integration in Eq. (18) yields the result that

$$I_2 = I_3 \tag{19}$$

Note that I_1 and I_4 do not depend on ϵ but I_2 and I_3 do. We can now write

$$\frac{D}{q_\infty} = \frac{D_1}{q_\infty} + \frac{D_2}{q_\infty} + \frac{1}{2\pi}\int_0^{2\pi} 2I_2 \mathrm{d}\epsilon \tag{20}$$

First Integration of I_2

The integral I_2 of Eq. (16) is integrable in algebraic terms. Write I_2 as

$$I_2 = -\frac{1}{2\pi}\int_0^L J(\eta, b-2f) S''(\eta)\mathrm{d}\eta \tag{21}$$

where

$$J(\eta, b-2f) = \int_0^L S''(\tau) \ell n\, |\tau - \eta - (b-2f)|\, \mathrm{d}\tau \tag{22}$$

Let

$$\left.\begin{aligned} \tau &= \frac{L}{2}(1+\cos\theta) \\ \eta &= \frac{L}{2}(1+\cos\phi) \\ S''(\tau) &= 12\pi \frac{r_0^2 \cos 2\theta}{L^2 \sin\theta} \end{aligned}\right\} \tag{23}$$

so that

$$J = 6\pi \frac{r_0^2}{L}\int_0^\pi \cos 2\theta \ell n\, |\cos\theta - \cos\phi - [2(b-2f)/L]|\, \mathrm{d}\theta \tag{24}$$

Integration by parts yields

$$\frac{J}{6\pi r_0^2/L} = \frac{1}{4}\int_0^\pi \frac{(\cos\theta - \cos 3\theta)}{\cos\theta - \cos\phi - \lambda}\mathrm{d}\theta \tag{25}$$

with

$$\lambda = 2(b-2f)/L \tag{26}$$

There are two cases in the integration of Eq. (25), depending on whether the denominator of the integral has a zero or not in the range of integration.

$$\begin{aligned} &\text{Case A: } \lambda + \cos\phi \leqq 1 \\ &\text{Case B: } \lambda + \cos\phi \geqq 1 \end{aligned} \tag{27}$$

Consider case A first. From the known result that

$$\int_0^\pi \frac{\cos n\theta \mathrm{d}\theta}{\cos\theta - \cos\phi} = \frac{\pi \sin n\phi}{\sin\phi} \tag{28}$$

it follows that

$$\int_0^\pi \frac{\cos n\theta \mathrm{d}\theta}{\cos\theta - \cos\phi - \lambda} = \frac{\pi \sin n\gamma}{\sin\gamma} \tag{29}$$

where

$$\cos\gamma = (\lambda + \cos\phi) \tag{30}$$

These results yield

$$\frac{J(\phi,\lambda)}{6\pi r_0^2/L} = \frac{\pi}{2}[1 - 2(\cos\phi + \lambda)^2]; \text{ case A} \tag{31}$$

Turning now to case B, consider the integral K_0 evaluated from integral tables

$$K_0 = \int_0^\pi \frac{\mathrm{d}\theta}{\cos\theta - (\cos\phi + \lambda)} = \frac{\pi}{[(\cos\phi + \lambda)^2 - 1]^{1/2}} \tag{32}$$

It follows readily that

$$K_1 = \int_0^\pi \frac{\cos\theta \mathrm{d}\theta}{\cos\theta - (\cos\phi + \lambda)} = \pi - \frac{\pi(\lambda + \cos\phi)}{[(\cos\phi + \lambda)^2 - 1]^{1/2}} \tag{33}$$

The following recursion formula is easily verified

$$K_{n+1} - K_{n-1} = 2(\lambda + \cos\phi)K_n, \qquad n \neq 0 \tag{34}$$

It follows, with the help of Eq. (24), that

$$\begin{aligned} \frac{J(\phi,\lambda)}{6\pi r_0^2/L} &= \frac{\pi}{2}[1 - 2(\lambda + \cos\phi)^2] \\ &+ \pi(\lambda + \cos\phi)[(\lambda + \cos\phi)^2 - 1]^{1/2} \end{aligned} \tag{35}$$

Second Integration of I_2

It is noted that the first term of $J(\phi,\lambda)$ is the same for cases A and B but that the second term is valid over the range $0 \leqq \phi \leqq \gamma$ where

$$\gamma = \cos^{-1}(1 - \lambda) \tag{36}$$

Accordingly,

$$\begin{aligned} 2\pi I_2 &= -\int_0^L J(\phi,\lambda) S''(\eta)\mathrm{d}\eta \\ &= -\frac{\pi}{2}\left(\frac{6\pi r_0^2}{L}\right)^2 [M(\lambda) + N(\lambda)] \end{aligned} \tag{37}$$

where

$$M(\lambda) = \int_0^\pi [1 - (\lambda + \cos\phi)^2]\cos 2\phi \mathrm{d}\phi \tag{38}$$

$$N(\lambda) = 2\int_0^\gamma (\lambda + \cos\phi)[(\cos\phi + \lambda)^2 - 1]^{1/2}\cos 2\phi \mathrm{d}\phi \tag{39}$$

Now integrate $M(\lambda)$ and $N(\lambda)$. $M(\lambda)$ can be easily integrated to yield

$$M(\lambda) = -(\pi/2) \tag{40}$$

With this result, Eq. (20) becomes

$$\begin{aligned} \frac{D}{q_\infty} &= \frac{4D_1}{q_\infty} - \frac{1}{q_\infty}\frac{1}{2\pi}\int_0^{2\pi}\mathrm{d}\epsilon \int_0^\gamma \left(\frac{6\pi r_0}{L}\right)^2 (\cos\phi + \lambda) \\ &\times [(\cos\phi + \lambda)^2 - 1]^{1/2}\cos 2\phi \mathrm{d}\phi \end{aligned} \tag{41}$$

where D_1 is the drag of an isolated body. Converting to drag coefficient form,

$$\begin{aligned} C_D &= 4C_D - \frac{36\pi r_0^2}{L^2}\frac{1}{2\pi}\int_0^{2\pi}\mathrm{d}\epsilon \int_0^\gamma (\cos\phi + \lambda) \\ &\times [(\cos\phi + \lambda)^2 - 1]^{1/2}\cos 2\phi \mathrm{d}\phi \end{aligned} \tag{42}$$

It is possible to give this result a simple physical meaning. If two bodies are superimposed so that they have zero lateral and longitudinal displacement from one another, then $b=a=0$. Also $\lambda=0$ and $\gamma=0$ deg, and the integral is zero. The drag of the configuration is that of a body of revolution with the cross-sectional area distribution of two bodies superimposed, or $4C_{D_l}$. Thus the second term of Eq. (28) represents favorable drag interference as a result of displacing the bodies laterally, longitudinally, or both.

It is now necessary to determine the value of the integral

$$R=\int_0^{\gamma}[(\cos\phi+\lambda)^2-1]^{1/2}(\cos\phi+\lambda)\cos 2\phi\,d\phi \tag{43}$$

The substitution

$$t=\lambda+\cos\phi \tag{44}$$

yields the result

$$R=\int_1^{1+\lambda} t(t^2-1)^{1/2}\left\{\frac{-1}{[1-(t-\lambda)^2]^{1/2}}-2[1-(t-\lambda)^2]^{1/2}\right\}dt \tag{45}$$

The integral can be reduced to Jacobian elliptic function form by the substitution

$$t=-1+[(\lambda+2)/(1-\alpha^2 sn^2 u)] \tag{46}$$

where sn^2u is the Jacobian elliptical sine amplitude function. Using the tables of Ref. 4, after much algebra, for $0\leqq\lambda\leqq 2.0$

$$R=\frac{\lambda}{3}(5-\lambda^2)E\left(\frac{\lambda}{2}\right)-\frac{\lambda}{6}(4-\lambda^2)K\left(\frac{\lambda}{2}\right) \tag{47}$$

Equation (38) can now be written

$$C_D=4C_{D_l}-\frac{8C_{D_l}}{\pi}\frac{1}{2\pi}\int_0^{2\pi}\left[\frac{\lambda}{3}(5-\lambda^2)E\left(\frac{\lambda}{2}\right)-\frac{\lambda}{6}(4-\lambda^2)K\left(\frac{\lambda}{2}\right)\right]d\epsilon \tag{48}$$

Since

$$\lambda=2/L(b-2\beta a\cos\epsilon) \tag{49}$$

the ϵ integration seems formidable. The integral was not evaluated in closed form but, instead, this last integration was done by computer. The integrand is perfectly regular, and the integral was evaluated by Simpson's rule. The equation contains both the transonic and supersonic results for the effect of lateral and longitudinal displacement on the wave drag of two-body combinations. The distribution of drag between the bodies is not given.

For $\lambda>2$, $R(\lambda)$ as given by the elliptic integrals, Eq. (47), is not valid. $R(\lambda)$ in this case must be defined by the definite integral, Eq. (43). Equation (48) should then be written

$$C_D=4C_{D_l}-\frac{8C_{D_l}}{\pi}\frac{1}{2\pi}\int_0^{2\pi}R(\lambda)\,d\epsilon \tag{50}$$

with the understanding that $R(\lambda)$ is defined by Eq. (43). For $\lambda\geq 2$, $R(\lambda)$ has been evaluated numerically, and the results are given in Table 1 for use in Eq. (50). The case $\lambda>2$ occurs when the nose of the rear body is behind the Mach forecone arising at the trailing edge of the forward body.

Illustrative Transonic Results

Some wave drag results at transonic speeds are now presented. These results are obtained from Eqs. (48) and (49) on the basis of the assumption that $M_\infty=1.0$. Then

$$\lambda=2b/L \tag{51}$$

Equation (48) then becomes

$$\frac{C_D}{C_{D_l}}=4-\frac{8}{\lambda}\left[\frac{\lambda}{3}(5-\lambda^2)E\left(\frac{\lambda}{2}\right)-\frac{\lambda}{6}(4-\lambda^2)K\left(\frac{\lambda}{2}\right)\right]\quad\lambda\leqq 2 \tag{52}$$

The first point to be noted is that C_D does not now depend on lateral spacing. Since the Mach waves are now planes normal to the body axis, the area distributions do not depend on the body lateral spacing. Consequently C_D is independent of spacing.

Some elucidation of this point is of interest. In point of fact, it is not really to be supposed that the drag of two bodies with no longitudinal displacement and purely lateral displacement should be unchanged for all lateral displacement. Some data of Drougge[3] on this effect are shown in Fig. 2. These data represent the wave drag of a parabolic body in the presence of another such body at $M_\infty=1.0$ and $M_\infty=1.15$. For $M_\infty=1$, it is noted that a minimum lateral spacing a/L of about 0.25 is needed before the total drag falls about 10%. This result is interpreted to mean that if $2a/L<0.25$, the effect of lateral displacement on wave drag is not significant. Such arrangements of stores with small gaps are feasible. Dashed lines in the figure represent the theory which will be discussed later.

Table 1 Tabulation of $R(\lambda)$; $\lambda\geq 2.0$

λ	$R(\lambda)$	λ	$R(\lambda)$
2.0	0.6667	3.5	0.7827
2.1	0.7283	3.6	0.7831
2.2	0.7479	3.7	0.7833
2.3	0.7586	3.8	0.7836
2.4	0.7653	3.9	0.7838
2.5	0.7699	4.0	0.7840
2.6	0.7731	4.1	0.7841
2.7	0.7755	4.2	0.7842
2.8	0.7772	4.3	0.7843
2.9	0.7786	4.4	0.7845
3.0	0.7797	4.5	0.7845
3.1	0.7806	4.6	0.7846
3.2	0.7813	4.7	0.7847
3.3	0.7819	4.8	0.7848
3.4	0.7823	4.9	0.7848
		5.0	0.7849
		∞	0.7854

Table 2 Values of $\Delta C_D/C_{D_l}$ for two Sears-Haack bodies at transonic speeds

b/L	$\Delta C_D/C_{D_l}$	b/L	$\Delta C_D/C_{D_l}$
0	2.000	1.1	0.0955
0.05	1.601	1.2	0.0512
0.10	1.210	1.3	0.0313
0.15	0.8337	1.4	0.0209
0.20	0.4795	1.5	0.0145
0.25	0.1541	1.6	0.0104
0.30	−0.1360	1.7	0.0079
0.40	−0.5870	1.8	0.0059
0.50	−0.8360	1.9	0.0046
0.60	−0.8594	2.0	0.0036
0.70	−0.6598		
0.80	−0.2783		
0.90	0.1732		
1.00	0.3023		

Equation (52) yields the dependence of total wave drag C_D on the longitudinal displacement. The total drag coefficient C_D of the pair of bodies as a multiple of the drag of a single body is shown in Fig. 3. At $b=0$ the wave drag is doubled due to mutual interference. At b/L between 0.5 and 0.6 the minimum wave drag of the combination occurs. At b/L of unity the drag coefficient ratio is $4-16/3\pi$, or 2.30. A pressure field acts behind the first body so that the interference between bodies is not zero. However, for $b/L>1$, the interference rapidly approaches zero as the distance between bodies increases. In this region, the values of $R(\lambda)$ given in Table 1 are applicable. One point of interest is that for $a=0$, $\lambda=2a\beta/L$ is independent of Mach number, so that Fig. 3 is also applicable at supersonic speeds for no lateral displacement.

The two-body results are applicable to arrangements of three or more bodies. A simple means of accounting for all interference terms is furnished by a simple squaring operation. Consider bodies A, B, and C, and form the following expression

$$(A+B+C)^2=A^2+B^2+C^2+(AB+BA)$$
$$+(AC+CA)+(BC+CB) \tag{53}$$

Interpret the expressions in the following manner. The term A^2 means the effect of A on A, and it represents the drag of body A alone; similarly for B^2 and C^2. The term AB is the interference of body A on body B, and BA is the interference of body B on body A. Thus $(AB+BA)$ represents the mutual interference between bodies A and B and depends only on the spacing between A and B independent of body C. To obtain

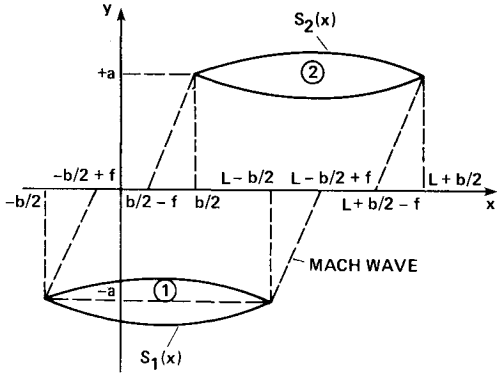

Fig. 1 Geometry and Mach waves for two bodies of revolution with lateral and longitudinal displacement.

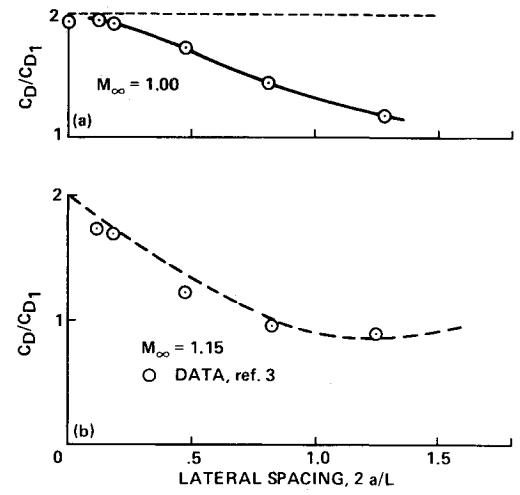

Fig. 2 Effect of lateral spacing on wave drag of a parabolic-arc body of revolution. a) $M_\infty=1.0$; b) $M_\infty=1.15$.

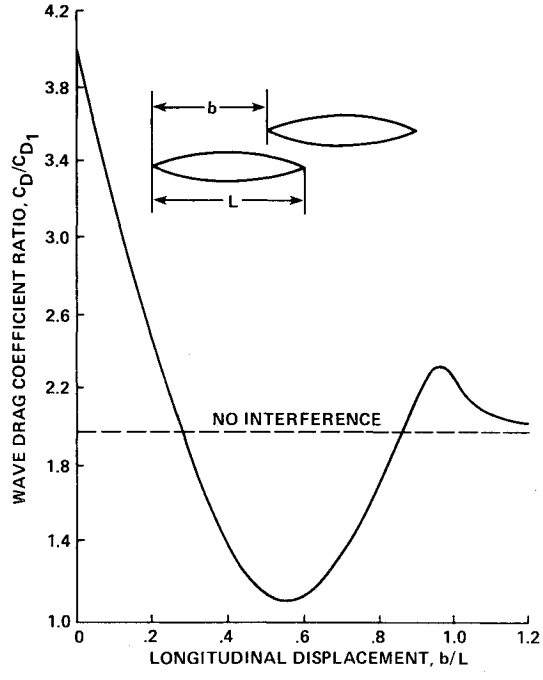

Fig. 3 Effect of longitudinal spacing on wave drag of two bodies at transonic speeds.

Table 3 Values of $\Delta C_D/C_{D_1}$ for two Sears-Haack bodies at supersonic speeds

	$2\alpha\beta/L\rightarrow$												
$b/L\downarrow$	0	0.1	0.2	0.3	0.4	0.5	0.6	0.7	0.8	0.9	1.0	1.1	1.2
0	2.00	1.495	1.015	0.585	0.225	−0.045	−0.213	−0.273	−0.232	−0.115	0	0	0
0.1	1.210	1.225	0.923	0.553	0.232	−0.017	−0.169	−0.224	−0.190	−0.109	−0.052	0	0
0.2	0.479	0.508	0.593	0.451	0.240	0.066	−0.044	−0.086	−0.091	−0.123	−0.107	−0.052	0
0.3	−0.136	−0.095	0.026	0.221	0.238	0.183	0.135	0.085	−0.022	−0.090	−0.118	−0.096	−0.043
0.4	−0.588	−0.537	−0.388	−0.149	0.161	0.297	0.300	0.193	0.076	−0.020	−0.083	−0.114	−0.097
0.5	−0.836	−0.780	−0.615	−0.357	−0.033	0.292	0.344	0.282	0.176	0.071	−0.019	−0.080	−0.102
0.6	−0.860	−0.804	−0.643	−0.402	−0.143	0.051	0.269	0.318	0.260	0.167	0.065	−0.020	−0.078
0.7	−0.660	−0.614	−0.490	−0.346	−0.260	−0.124	0.050	0.253	0.298	0.245	0.162	0.065	−0.016
0.8	−0.278	−0.260	−0.249	−0.309	−0.300	−0.232	−0.112	0.049	0.236	0.281	0.233	0.151	0.058
0.9	0.173	0.105	−0.091	−0.212	−0.271	−0.268	−0.210	−0.101	0.047	0.226	0.272	0.228	0.142
1.0	0.302	0.209	0.059	−0.083	−0.187	−0.243	−0.244	−0.193	−0.094	0.044	0.213	0.259	0.214
1.1	0.096	0.127	0.143	0.042	−0.075	−0.169	−0.222	−0.226	−0.181	−0.089	0.042	0.203	0.248
1.2	0.051	0.057	0.091	0.113	0.033	−0.069	−0.156	−0.207	−0.209	−0.168	−0.082	0.041	0.196
1.3	0.031	0.034	0.042	0.073	0.046	0.027	−0.065	−0.146	−0.192	−0.198	−0.161	−0.080	0.043
1.4	0.021	0.022	0.026	0.034	0.063	0.085	0.024	−0.061	−0.136	−0.183	−0.186	−0.151	−0.074

the wave drag of the combination of all three bodies, we need only to add up the terms of Eq. (53).

The actual mutual interference term in Eq. (50) is represented by

$$\frac{\Delta C_D}{C_{D_1}} = 2 - \frac{8}{\pi}\frac{1}{2\pi}\int_0^{2\pi} R(\lambda)\,d\epsilon \tag{54}$$

This expression has been evaluated for a series of values of b/L using $R(\lambda)$ from Table 1 and Eq. (47). The resulting table of mutual interference factors, given as Table 2, is for use in determining the wave drag of various arrangements of Sears-Haack bodies at transonic speeds.

Consider now an arrangement of three Sears-Haack bodies as shown in Fig. 4. The calculation of the wave drag of this arrangement along the lines discussed above is shown in the figure. It is noted that the drag of the three-body arrangement has the total drag of 1.63 bodies. The drag reduction comes about through highly favorable mutual interference between bodies A and B and B and C.

It is easy to generalize the above results to n bodies, which are added in the downstream direction following the pattern of Fig. 4. It is readily shown that

$$C_D/C_{D_1} = n - (n-1)(0.836) + (n-2)(0.302) \tag{55}$$

It has been assumed that for $b/L > 1.5$, the mutual interference is negligible in accordance with Table 2; thus,

$$C_D/C_{D_1} = 0.466n + 0.232 \tag{56}$$

$$C_D/nC_{D_1} = 0.466 + 0.232/n \tag{57}$$

n	C_D/C_{D_1}	C_D/nC_{D_1}
3	1.630	0.543
4	2.096	0.524
5	2.562	0.512
6	3.028	0.505
∞	∞	0.466

If two bodies are displaced longitudinally to the optimal position, the total drag is 1.12 (Fig. 3) times the drag of the one body alone, yielding a reduction in wave drag of 44% due to mutual interference. If more bodies are to be used, further reduction in drag can be accomplished. For six bodies a 49.5% reduction in wave drag can be accomplished. For a much larger number of bodies, a theoretical limit of 53.4% reduction in wave drag is possible using the above scheme of arrangement.

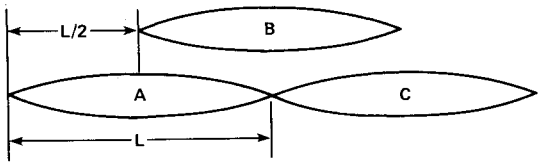

	(b/L)	$\Delta C_D/C_{D_1}$
A^2	–	1
B^2	–	1
C^2	–	1
(AB + BA)	0.5	-0.836
(AC + CA)	1.0	0.302
(BC + CB)	0.5	-0.836
C_D/C_{D_1} =		1.630
$C_D/3C_{D_1}$ =		0.543

Fig. 4 Calculation of the transonic wave drag of a three-body arrangement of Sears-Haack bodies.

Now contrast the above case with that for a triple ejection rack, in which three stores are mounted on one rack so that they have no longitudinal displacement. Accordingly, their drag is equal to that of nine bodies alone. Thus there is a 300% increase in drag that can be contrasted with the 45.7% reduction of drag possible with the arrangement of Fig. 4.

Many arrangements of external stores are possible by using various combinations of lateral and longitudinal displacement. These arrangements can be readily analyzed by the preceding method to determine the total wave drag.

Several cautions are in order concerning the above results. First, it is assumed that the flow is attached to the bodies to their trailing edges and no viscous wake occurs. However, the boundary layer can separate before the trailing edge so that the predicted values may be in error. In the second place, we have neglected skin friction that may change as a result of the interference pressure distributions. Third, the external stores interact with the airplane to cause an increment in airplane drag associated with either pressure drag or skin friction.

Illustrative Supersonic Effects

The transonic results shown in the previous section are limiting results of the supersonic area rule as the Mach number approaches unity. For the supersonic area rule, the drag results depend in a nondimensional manner only on b/L and $2\alpha\beta/L$ as follows:

$$\frac{C_D}{(r_0/L)^2} = F(b/L,\ 2a\beta/L) \tag{58}$$

Equation (58) has been evaluated for a range of values of the two parameters, and the results have been tabulated in terms of the mutual interference factor, $\Delta C_D/C_{D_1}$. Similarly as in Table 2 for M_∞ of unity, these results are listed in Table 3 for supersonic speed. The values in the table have been obtained on an IBM PC-XT by double integration using Simpson's rule and Eqs. (43) and (54).

Table 3 is now used to illustrate the effect of lateral spacing on the total wave drag of two bodies with no longitudinal displacement. The result is shown vs the nondimensional lateral spacing $2\beta a/L$ in Fig. 5. It is noted that for values of the parameter above 0.5, the mutual interference is favorable. This result follows from the facts that the nose Mach wave from one body intersects the other body behind its half-length

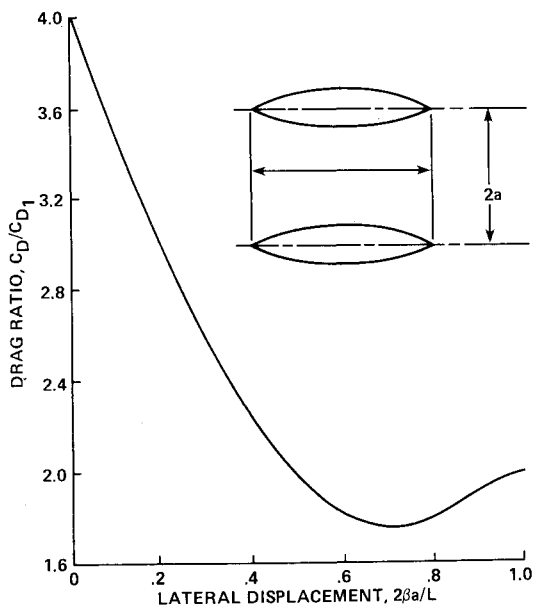

Fig. 5 Effect of lateral spacing on the total drag of a two-body arrangement.

position and the positive pressure behind the wave causes thrust on the rearward sloping surface of the body. For values of $2\beta a/L$ greater than unity, the two bodies are not within the zones of influence of one another, and the mutual interference is zero.

The figure shows a drag saving of 12% of the drag of the bodies alone for a value of $2\beta a/L$ of about 0.7. If it is assumed that the store is mounted under a wing which acts as a flat reflection plane, then the store would have to be a distance from the reflection plane of half this value. For $M_\infty = (2)^{1/2}$, the distance from the reflection plane would be about 35% of the body length. For higher Mach numbers the distances would be less.

For a store mounted tangent to a reflection surface, Fig. 5 shows that its wave drag is twice the body-alone value. If, however, the body is semisubmerged in the reflection plane, its drag is half that of a body alone. These results will be modified to some degree by the presence of the boundary layer on the reflection surface. Both the skin friction of the body and reflection plane can be affected. This effect bears future investigation.

The regions of favorable interference can be shown using the results of Table 3. The values in this table are good to two decimal points and in most cases to three decimal points. Contours of constant $\Delta C_D/C_{D_1}$ are shown in Fig. 6 for ranges of $2\beta a/L$ and b/L. A region of favorable interference exists for large lateral spacing and small longitudinal spacing. In this region the positive pressure from the front of each body acts on the back of the other body producing thrust. Above the upper Mach line the bodies do not interfere with one another.

A second region of favorable interference exists for ranges of spacings as shown in the figure. For small lateral spacings and a longitudinal spacing near 0.5, the interference is most favorable. Behind this region of favorable interference a region of slightly adverse interference exists.

As another example of how the total wave drag of a pair of bodies depends on their relative positions, the case is considered of a body moving obliquely between the forward and rearward Mach waves of the forward body as in Fig. 7. The wave drag interference is always adverse in this case.

Now consider an example of a variable three-body array as shown in Fig. 8. The laterally spaced body is moved in the longitudinal direction to find its position of minimum wave drag. For spacings $2\beta a/L$ of 0 and 0.2, the optimum value of b/L is close to 0.5. For $2\beta a/L = 0.4$, the curve is flat so that no significant penalty occurs in using b/L of 0.5.

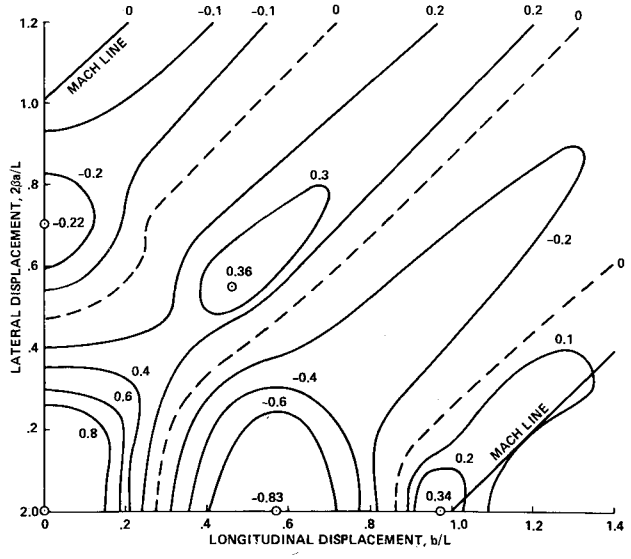

Fig. 6 Contours of constant wave drag ratio $\Delta C_D/C_{D_1}$ for two Sears-Haack bodies based on Table 3.

It is of interest how the drag of an array of bodies with minimum wave drag at one Mach number changes as the Mach number increases. Consider the foregoing case of three bodies. Let the lateral spacing $2a/L$ be 30% of the body length. As the Mach number increases, the value of $2\beta a/L$ increases. The wave drag also increases relative to that for the bodies alone. For three bodies, Fig. 9 shows that the total wave drag is about half that for three bodies alone at $M_\infty = 1.0$, but that it increases asymptotically approaching unity as M_∞ increases. The wave drag interference is favorable at all supersonic Mach numbers.

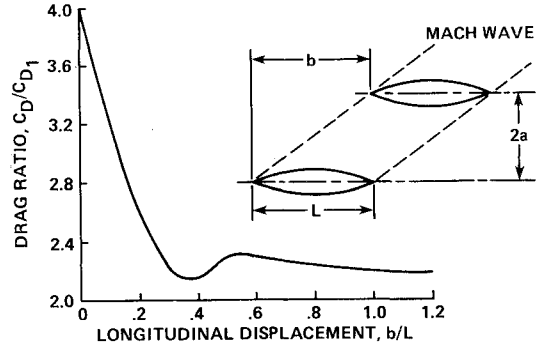

Fig. 7 Total wave drag of two bodies with the rear body within the Mach waves of the front body.

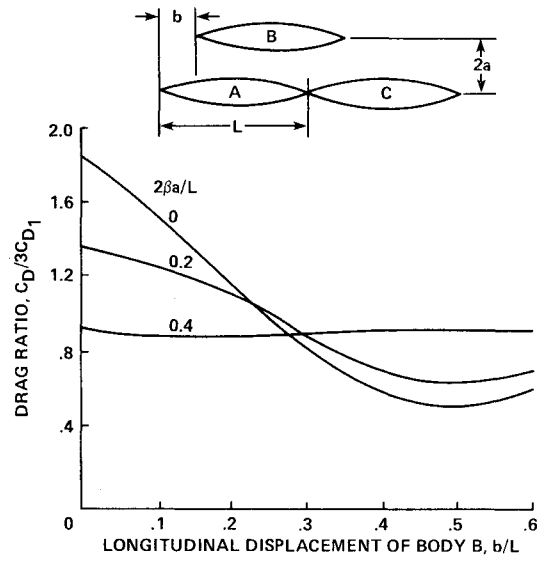

Fig. 8 Wave drag of a variable geometry three-body array.

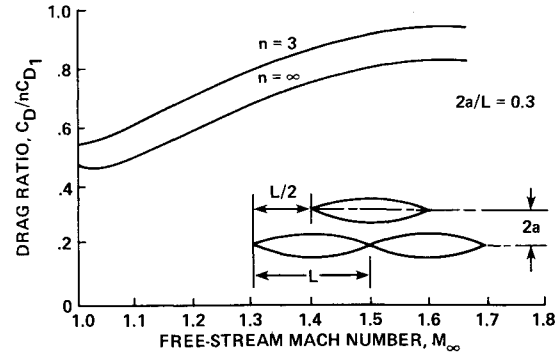

Fig. 9 Relationships between Mach number and wave drag of many-body arrays.

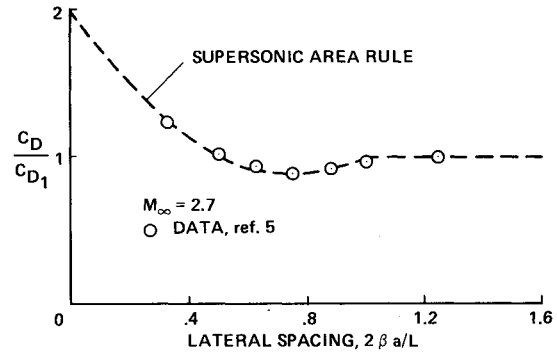

Fig. 10 Effect of lateral spacing on the wave drag of one of a pair of Sears-Haack bodies at $M_\infty = 2.7$.

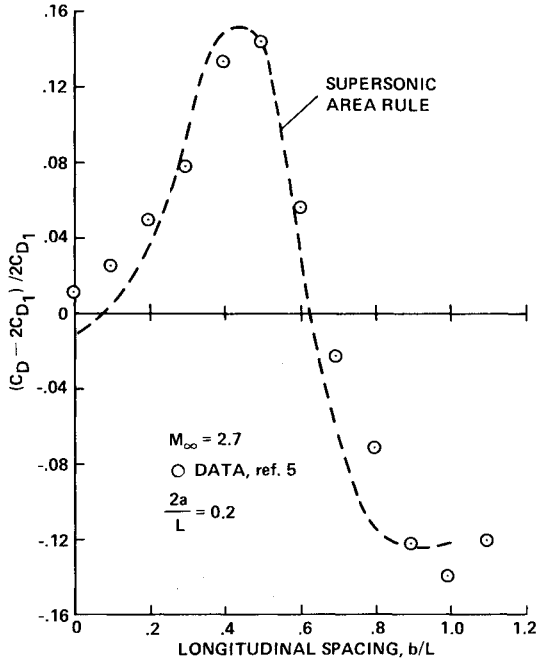

Fig. 11 Effect of longitudinal spacing on the interference wave drag of a pair of Sears-Haack bodies at $M_\infty = 2.7$.

It is easy to determine the wave drag for an infinite alternating array of bodies based on the three-body array shown in Fig. 9. The result marked by $n = \infty$ in the figure shows further drag reduction over the three-body array. Using the results of Table 3, it is possible to determine the effect of a reflection plane on the results of Fig. 9, but the calculation has not been carried out.

Comparison Between Data and Theory

The first comparison between data and theory is made in Fig. 2 for $M_\infty = 1.0$ and $M_\infty = 1.15$. The data are for parabolic-arc bodies separated laterally and the theory is for Sears-Haack bodies. The theory is represented by the dashed curves in the figure. The null effect of lateral spacing for $M_\infty = 1.0$ has already been discussed. At $M_\infty = 1.15$, the data and theory are in good agreement. This result suggests that the difference is small between the wave drag characteristics of a pair of parabolic-arc bodies and a pair of Sears-Haack bodies of equal thickness ratio.

Wave drag data for a pair of Sears-Haack bodies are available in Ref. 5 for $M_\infty = 2.7$ as determined by pressure distribution. In Fig. 10 data are compared with theory for the effects of lateral spacing and in Fig. 11 for longitudinal spacing. Figure 10 shows the ratio of the wave drag of one of the bodies including interference to that with no interference. The agreement between the data and the supersonic area rule is quite good. In Ref. 5 Bantle suggests adjusting the value of β in the theory so that the theoretical Mach wave direction coincides with that of the nose shock wave. However, since a Sears-Haack body has a blunt nose, an experimental value of the nose shock angle should be used for this adjustment. This adjustment, not shown in Fig. 10, further improves the agreement between data and theory. The good agreement between data and experiment for the wave drag ratio shown in the figure does not imply that slender-body theory accurately predicts the absolute wave drag. In fact, in this case it does not.

The data in Fig. 11 represent results for two Sears-Haack bodies separated by 20% of the body length at $M_\infty = 2.7$. It is noted that for $2a/L = 0.2$ the maximum favorable interference occurs at a value of b/L of about 1.0 instead of 0.5 at $2a/L = 0$. The agreement between data and theory is considered acceptable in view of uncertainties in the data as well as in the numerical calculations for the supersonic area rule.

Further Considerations

The present analysis is fairly specific in that it deals only with Sears-Haack bodies. It can be extended to other types of bodies which are also pointed at both ends. Bodies with blunt bases can also be treated, but consideration must be given to base drag.

For two bodies, the pressure field of one body will change the pressure just before the base of the other body, and the base drag must be corrected for this effect. The change in base drag can be considered part of the mutual interference in the usual way. The pressure coefficient contains squared terms in slender-body theory and, as such, is not strictly additive for many bodies. However, this fact can probably be ignored for most practical purposes and the superposition carried out as in the present method.

Another way in which the mutual interference between two bodies can be obtained is through the use of panel methods. Systematic calculations must be made as a function of longitudinal and lateral spacing at a fair cost in computer time. However, this is a good way of handling empennage effects.

One question that naturally arose in the course of the present work is how skin friction and boundary-layer separation are influenced by mutual interference between two bodies. The body pressure distribution can be approximated by linearly combining pressure distributions. The skin friction and separation of the body boundary layer can then be studied using integral methods. Such an approach should show the importance of mutual interference on skin friction and separation.

The complete assessment of drag of a store-airframe combination must include consideration of the effect of the store on the airframe pressure drag and skin friction. While the supersonic area rule can be used to treat the wave drag of the store-airframe combination, a panel method will separate out the components of mutual interference.

The influence of the store (or stores) on the viscous drag of the airframe is a difficult problem, particularly for closely coupled stores. Considering only a planar reflection plane, we encounter a three-dimensional problem in shock-wave/boundary-layer interaction. To calculate the effects, one may need to invoke the Navier-Stokes equation. For closely coupled stores such as semisubmerged bodies, this possibility appears real.

Concluding Remarks

This paper addresses the problem of finding minimum wave drag arrays of Sears-Haack bodies, with special reference to external stores. The problem of the mutual interference

among bodies has been solved. The interference of an airframe on an array of Sears-Haack bodies has also been solved to the degree of approximation that the airframe (wing) can be modeled by a planar reflection surface.

References

[1]Carmichael, R. I. and Erickson, L. L., "PAN AIR—A Higher Order Panel Method for Predicting Subsonic or Supersonic Linear Potential Flows About Arbitrary Configurations," AIAA Paper 81-1255, 1981.

[2]Nielsen, J. N., *Missile Aerodynamics*, McGraw-Hill Book Co., Inc., New York, 1960, pp. 269-271 and 296-302.

[3]Drougge, Georg, "An Experimental Investigation of the Interference Between Bodies of Revolution at Transonic Speeds with Special Reference to the Sonic and Supersonic Area Rules," The Aeronautical Research Institute of Sweden, Report 83, Oct. 1958.

[4]Byrd, P. F. and Friedman, M. D., *Handbook of Elliptic Integrals for Engineers and Scientists*, rev. ed., Springer-Verlag, New York, 1971.

[5]Bantle, J. W., "Analysis of the Interference Effects Between Two Sears-Haack Bodies at Mach 2.7," Engineering and Applied Sciences Thesis, George Washington University, Washington, DC, 1982.